



Corrigendum

Corrigendum to “Determination of the top-quark pole mass and strong coupling constant from the $t\bar{t}$ production cross section in pp collisions at $\sqrt{s} = 7$ TeV” [Phys. Lett. B 728 (2014) 496–517]



CMS Collaboration

CERN, Switzerland

ARTICLE INFO

Article history:

Received 19 August 2014

Accepted 19 August 2014

Available online 23 August 2014

Editor: M. Doser

Table 2
Results obtained for m_t^{pole} by comparing the measured $t\bar{t}$ cross section to the NNLO+NNLL prediction with different NNLO PDF sets. The total uncertainties account for the full uncertainty on the measured cross section ($\sigma_{t\bar{t}}^{\text{meas}}$), the PDF and scale ($\mu_{R,F}$) uncertainties on the predicted cross section, the uncertainties of the $\alpha_S(m_Z)$ world average and of the LHC beam energy (E_{LHC}), and the ambiguity in translating the MC-generator based mass dependence (m_t^{MC}) of the measured cross section into the pole-mass scheme.

	m_t^{pole} (GeV)	Uncertainty on m_t^{pole} (GeV)						m_t^{MC}
		Total	$\sigma_{t\bar{t}}^{\text{meas}}$	PDF	$\mu_{R,F}$	α_S	E_{LHC}	
ABM11	172.7	+3.2 −3.1	+1.8 −1.8	+2.2 −2.0	+0.7 −0.7	+1.0 −1.0	+0.8 −0.8	+0.4 −0.3
CT10	177.0	+3.6 −3.3	+2.2 −2.1	+2.4 −2.0	+0.9 −0.9	+0.8 −0.8	+0.9 −0.9	+0.5 −0.4
HERAPDF1.5	179.5	+3.5 −3.2	+2.4 −2.2	+1.7 −1.5	+0.9 −0.8	+1.2 −1.1	+1.0 −1.0	+0.6 −0.5
MSTW2008	177.9	+3.2 −3.0	+2.2 −2.1	+1.6 −1.4	+0.9 −0.9	+0.9 −0.9	+0.9 −0.9	+0.5 −0.5
NNPDF2.3	176.7	+3.0 −2.8	+2.1 −2.0	+1.5 −1.3	+0.9 −0.9	+0.7 −0.7	+0.9 −0.9	+0.5 −0.4

By mistake, an incorrect (too large) value was used for the uncertainty on the measured top-quark pair cross section. Taking the correct relative uncertainty of 4.1%, which was also quoted in Section 4 of the paper, has the following consequences:

- The uncertainty bands in the illustration of the measured cross section as a function of the top-quark mass, m_t , and of the strong coupling constant, $\alpha_S(m_Z)$, are narrower. The corrected versions are provided in Fig. 1.
- The confidence intervals for m_t and $\alpha_S(m_Z)$ obtained from the posterior densities become narrower. The corrected examples are shown in Fig. 3.

- While the central values of the results for m_t and $\alpha_S(m_Z)$ remain the same within the numerical precision of the computation, their total uncertainties decrease. Our main results, obtained with the NNPDF2.3 set of parton distribution functions (PDFs) at next-to-next-to-leading order, become $m_t = 176.7^{+3.0}_{-2.8}$ GeV (was $^{+3.8}_{-3.4}$ GeV) and $\alpha_S(m_Z) = 0.1151^{+0.0028}_{-0.0027}$ (was $^{+0.0033}_{-0.0032}$). The corrected results for all five PDF sets are given in the revised Tables 2 and 3 and illustrated in the revised Figs. 4 and 5. Only the numbers in the third and fourth columns in these tables have changed. The experimental uncertainties on m_t and $\alpha_S(m_Z)$ decrease significantly. However, they remain the largest contribution.

DOI of original article: <http://dx.doi.org/10.1016/j.physletb.2013.12.009>.

E-mail address: cms-publication-committee-chair@cern.ch.

The general conclusions of the paper are unchanged.

<http://dx.doi.org/10.1016/j.physletb.2014.08.040>

0370-2693/© 2014 CERN for the benefit of the CMS Collaboration. Published by Elsevier B.V. This is an open access article under the CC BY license (<http://creativecommons.org/licenses/by/3.0/>). Funded by SCOAP³.

Table 3

Results obtained for $\alpha_S(m_Z)$ by comparing the measured $t\bar{t}$ cross section to the NNLO+NNLL prediction with different NNLO PDF sets. The total uncertainties account for the full uncertainty on the measured cross section ($\sigma_{t\bar{t}}^{\text{meas}}$), the PDF and scale ($\mu_{R,F}$) uncertainties on the predicted cross section, the uncertainty assigned to the knowledge of m_t^{pole} , and the uncertainty of the LHC beam energy (E_{LHC}).

	$\alpha_S(m_Z)$	Uncertainty on $\alpha_S(m_Z)$					
		Total	$\sigma_{t\bar{t}}^{\text{meas}}$	PDF	$\mu_{R,F}$	m_t^{pole}	E_{LHC}
ABM11	0.1187	+0.0024 -0.0024	+0.0013 -0.0015	+0.0015 -0.0014	+0.0006 -0.0005	+0.0010 -0.0010	+0.0006 -0.0006
CT10	0.1151	+0.0030 -0.0029	+0.0018 -0.0018	+0.0018 -0.0016	+0.0008 -0.0007	+0.0012 -0.0013	+0.0007 -0.0007
HERAPDF1.5	0.1143	+0.0020 -0.0020	+0.0012 -0.0013	+0.0010 -0.0009	+0.0005 -0.0004	+0.0010 -0.0010	+0.0006 -0.0006
MSTW2008	0.1144	+0.0026 -0.0027	+0.0017 -0.0018	+0.0012 -0.0011	+0.0008 -0.0007	+0.0012 -0.0013	+0.0007 -0.0008
NNPDF2.3	0.1151	+0.0028 -0.0027	+0.0017 -0.0018	+0.0013 -0.0011	+0.0009 -0.0008	+0.0013 -0.0013	+0.0008 -0.0008

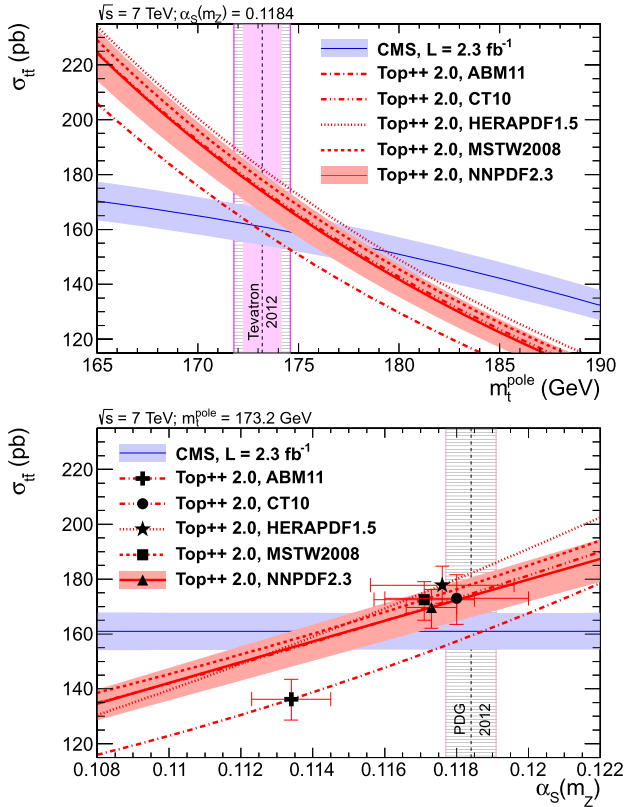


Fig. 1. Predicted $t\bar{t}$ cross section at NNLO+NNLL, as a function of the top-quark pole mass (top) and of the strong coupling constant (bottom), using five different NNLO PDF sets, compared to the cross section measured by CMS assuming $m_t = m_t^{\text{pole}}$. The uncertainties on the measured $\sigma_{t\bar{t}}$ as well as the renormalization and factorization scale and PDF uncertainties on the prediction with NNPDF2.3 are illustrated with filled bands. The uncertainties on the $\sigma_{t\bar{t}}$ predictions using the other PDF sets are indicated only in the bottom panel at the corresponding default $\alpha_S(m_Z)$ values. The m_t^{pole} and $\alpha_S(m_Z)$ regions favored by the direct measurements at the Tevatron and by the latest world average, respectively, are shown as hatched areas. In the top panel, the inner (solid) area of the vertical band corresponds to the original uncertainty of the direct m_t average, while the outer (hatched) area additionally accounts for the possible difference between this mass and m_t^{pole} .

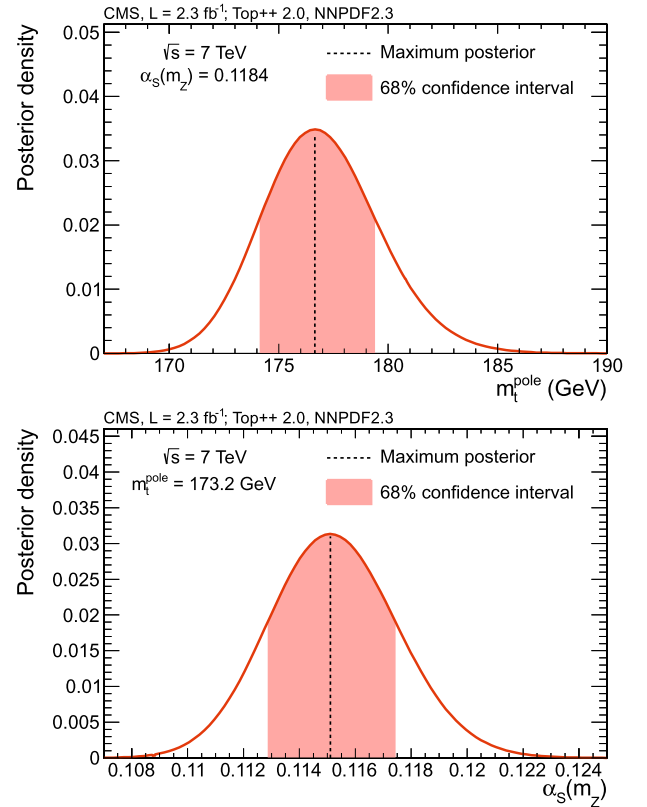


Fig. 3. Marginal posteriors $P(m_t^{\text{pole}})$ (top) and $P(\alpha_S)$ (bottom) based on the cross section prediction at NNLO+NNLL with the NNLO parton distributions from NNPDF2.3. The posteriors are constructed as described in the text. Here, $P(m_t^{\text{pole}})$ is shown for $\alpha_S(m_Z) = 0.1184$ and $P(\alpha_S)$ for $m_t^{\text{pole}} = 173.2 \text{ GeV}$.

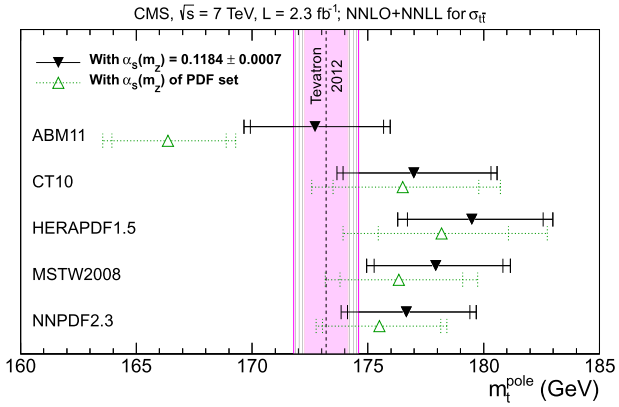


Fig. 4. Results obtained for m_t^{pole} from the measured $t\bar{t}$ cross section together with the prediction at NNLO+NNLL using different NNLO PDF sets. The filled symbols represent the results obtained when using the $\alpha_s(m_Z)$ world average, while the open symbols indicate the results obtained with the default $\alpha_s(m_Z)$ value of the respective PDF set. The inner error bars include the uncertainties on the measured cross section and on the LHC beam energy as well as the PDF and scale uncertainties on the predicted cross section. The outer error bars additionally account for the uncertainty on the $\alpha_s(m_Z)$ value used for a specific prediction. For comparison, the latest average of direct m_t measurements is shown as vertical band, where the inner (solid) area corresponds to the original uncertainty of the direct m_t average, while the outer (hatched) area additionally accounts for the possible difference between this mass and m_t^{pole} .

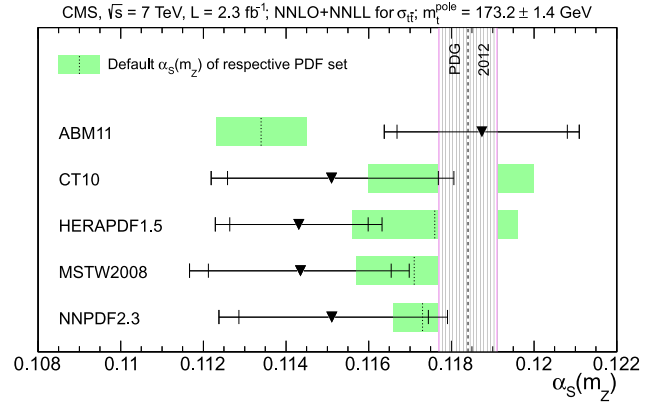


Fig. 5. Results obtained for $\alpha_s(m_Z)$ from the measured $t\bar{t}$ cross section together with the prediction at NNLO+NNLL using different NNLO PDF sets. The inner error bars include the uncertainties on the measured cross section and on the LHC beam energy as well as the PDF and scale uncertainties on the predicted cross section. The outer error bars additionally account for the uncertainty on m_t^{pole} . For comparison, the latest $\alpha_s(m_Z)$ world average with its uncertainty is shown as a hatched band. For each PDF set, the default $\alpha_s(m_Z)$ value and its uncertainty are indicated using a dotted line and a shaded band.